

# Valence- and Dipole-Bound Anions of the Thymine–Water Complex: Ab Initio Characterization of the Potential Energy Surfaces<sup>†</sup>

Tomaso Frigato, Daniel Svozil,\* and Pavel Jungwirth

*Institute of Organic Chemistry and Biochemistry, Academy of Sciences of the Czech Republic, and Center for Biomolecules and Complex Molecular Systems, Flemingovo nám. 2, 166 10, Prague 6, Czech Republic*

*Received: July 25, 2005; In Final Form: November 14, 2005*

The potential energy surfaces of the neutral and anionic thymine–water complexes are investigated using high-level ab initio calculations. Both dipole-bound (DB) and valence-bound (VB) anionic forms are considered. Four minima and three first-order stationary points are located, and binding energies are computed. All minima, for both anions, are found to be vertically and adiabatically stable. The binding energies are much higher for valence-bound than for dipole-bound anions. Adiabatic electron affinities are in the 66–287 meV range for VB anions and the 4–60 meV range for DB anions, and vertical detachment energies are in the 698–977 meV and 10–70 meV range for VB and DB anions, respectively. For cases where literature data are available, the computed values are in good agreement with previous experimental and theoretical studies. It is observed that electron attachment modifies the shape of the potential energy surfaces of the systems, especially for the valence-bound anions. Moreover, for both anions the size of the energy barrier between the two lowest energy minima is strongly reduced, rendering the coexistence of different structures more probable.

## 1. Introduction

Electron trapping by nucleotide bases has a crucial importance in understanding the mechanism of DNA-base damage due to high energy radiation. Radical anions resulting from electron attachment to DNA and RNA bases may participate in a chain of chemical reactions that can lead to a permanent alteration of the original bases. Generally, two different types of anions can be produced by an excess electron attachment.<sup>1</sup> A conventional one, called a valence-bound (VB) anion, is obtained when the excess electron occupies a valence molecular orbital. VB anions are characterized by significant changes in geometry upon the capture of the electron. The second type, usually referred to as a dipole-bound (DB) anion, is found in polar molecules that exhibit a large dipole moment in their neutral form. The minimum value of the dipole moment needed to bind an electron was first estimated by Fermi and Teller in 1947.<sup>2</sup> For molecular systems, this value depends on the molecular moment of inertia,<sup>3</sup> but as a rule of thumb the value 2.5 D is usually adopted.<sup>4</sup> In DB anions, the excess electron is loosely bound primarily because of the electrostatic charge-dipole interactions<sup>5–7</sup> and dispersion interactions<sup>8–11</sup> between the electron and the neutral molecule. The resulting anionic wave function is very diffuse, and only small geometrical relaxation occurs upon electron capture.

Electron attachment to DNA bases has been studied extensively, both experimentally and theoretically (for a recent review, see ref 12). It is usually described in terms of properties such as adiabatic electron affinity (AEA), vertical electron affinity (VEA), and vertical detachment energy (VDE).

Two main experimental techniques for the investigation of electronic properties of molecular anions are photoelectron spectroscopy (PES) and Rydberg electron-transfer spectroscopy

(RET). Recorded spectra of uracil (U) and thymine (T), obtained by PES<sup>13</sup> and RET experiments,<sup>5</sup> showed a typical feature of DB anions: a sharp, intense peak between 0 and 0.1 eV. This particular shape of the spectrum is a consequence of the fact that the attachment of an electron in a DB state does not perturb the geometry of the neutral precursor significantly. In a subsequent study, RET spectroscopy showed that it is possible to obtain a VB anion of isolated uracil by electron attachment to the Ar–U complex, followed by evaporation of argon.<sup>14</sup>

The first theoretical calculations of electron attachment on isolated uracil<sup>15</sup> and thymine<sup>16</sup> were restricted to dipole-bound anions only. Later, a first positive estimate of AEA for the thymine VB anion was calculated.<sup>17</sup> Recently, we have reinvestigated both valence- and dipole-bound anions of thymine at a high level of theory.<sup>18</sup> This work supported the previous evidence for the simultaneous existence of both DB and VB adiabatically stable anions of isolated thymine, with the VB anion having a small adiabatic but a large vertical stability. The DB to VB orbital electron transfer has been studied by Sommerfeld,<sup>19</sup> who postulated the possibility, for isolated uracil, of a decay of the higher energy VB state via a vibrationally excited DB state. For systems where the VB anion is the most stable, like hydrated DNA bases, DB states may act as “doorways” to the formation of VB anions.<sup>19</sup>

Hydration of nucleic acid bases is of fundamental importance because biological processes take place in an aqueous environment. A consistent number of studies have focused on the microhydration of uracil, which is the structurally simplest base. Neutral complexes composed of up to seven water molecules have been studied by ab initio<sup>20–23</sup> and DFT methods.<sup>24–31</sup> Recently, a system consisting of uracil and 49 H<sub>2</sub>O molecules has been investigated using ab initio molecular dynamics simulations,<sup>32</sup> raising interesting questions about the role of finite temperature and system size on DNA bases hydration. Thy-

<sup>†</sup> Part of the special issue “Jürgen Troe Festschrift”.

\* Corresponding author. E-mail: daniel.svozil@uochb.cas.cz.

mine–water complexes were considered as well in some of the aforementioned works.<sup>21,23</sup>

Regarding the composite effects of hydration and electron attachment, it was shown experimentally by Bowen et al.,<sup>33</sup> that the addition of a single water molecule strongly stabilizes the valence-bound anion of uracil. Very similar results were obtained for microhydrated thymine:<sup>34</sup> the onset of the PES spectrum for a singly hydrated thymine, corresponding to the AEA value, was found around 0.3 eV, while the maximum (VDE) was located around 0.9 eV.

The first theoretical calculations by Adamowicz et al.<sup>35</sup> failed to reproduce the stabilization effect of hydration on the valence-bound anion of uracil. Three structures, corresponding to three energy minima of the complex, were considered, and calculations converged to adiabatically and vertically stable DB anions in all configurations. The reason VB anions were not found is probably due to the fact that geometry optimizations were performed only at the HF level of theory. The addition of two water molecules allowed one to converge the calculations to a VB anion  $U-(H_2O)_3^-$ , the energy of which approached the energy of the neutral system,<sup>36</sup> although a still slightly negative value of the AEA was computed. This result is in disagreement with experimental findings.<sup>34</sup>

Ortiz et al.<sup>37</sup> performed calculations of the uracil–water complex at the MP2/6-311++G\*\* level of theory. Four minimal structures of the complex (plus three isomeric forms) were considered. Only valence-bound anions were obtained, and three out of the four minima were found to be adiabatically stable. Although these results are in better agreement with experiments than previous calculations, the authors anticipated that “larger basis sets and more complete correlation methods are likely to produce larger VDEs and AEAs”.<sup>37</sup>

VDEs of the same four  $U-H_2O$  complexes were computed by Gutowski et al.<sup>38</sup> The authors found that the level of theory used, B3LYP/6-31++G\*\*(5d), overestimates the VDE of bare uracil by approximately 200 meV and, therefore, they assumed that the same error may affect the results obtained for the hydrated uracil.

An interesting anionic form of the  $U-H_2O$  complex was discovered by Adamowicz et al.,<sup>39</sup> who found a structure (called AISE, anion with internally suspended electron) with the electron positioned between uracil and water; this structure has a high VDE but a quite large negative AEA and, therefore, can only exist as a metastable state that will interconvert to either a stable valence form of anion or that will lead to electron detachment.

To the best of our knowledge, only minimum energy configurations were considered so far in theoretical calculations of anionic hydrated uracil (or thymine); first-order transition states were characterized for the uracil–water complex,<sup>20</sup> but only in its neutral form. The energy barriers were found to be too high for thermal transitions between adjacent minima at room temperature.

In the present contribution, the methodology applied to isolated thymine previously<sup>18</sup> is used to investigate electronic affinities of the thymine–water complex. Combining the two studies, we present an accurate investigation of the influence on thymine of electron attachment, microhydration by a single water molecule, and microhydration and electron attachment at one time. Four minima and three transition-state structures are considered, and for all geometries both DB and VB anions are found. Moreover, energies of transition states of the neutral and anionic forms are determined to elucidate the role of electron

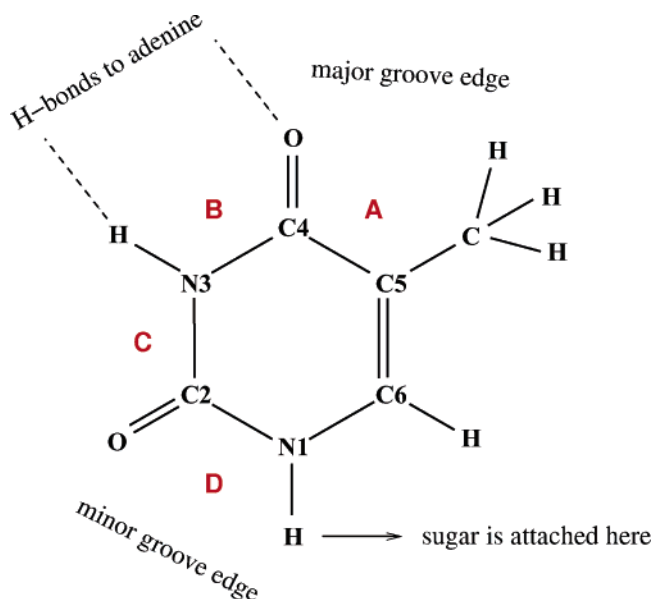


**Figure 1.** Chemical formula and atom numbering of thymine. Atoms of water are indicated in text as  $O_w$  and  $H_w$ . In nucleoside, the sugar is bonded to the N1 atom. Adenine is bonded to  $H-N3$  and  $O=C4$ . Minor and a major groove edges are indicated. Positions of water in our system are denoted with A, B, C, and D.

attachment on the shape of the potential energy surface of the thymine–water complex.

## 2. Methods

Figure 1 shows the structure and atom numbering of the thymine molecule; atoms of water are denoted in the text as  $O_w$  and  $H_w$ . First, four minimum energy structures, obtained exploring the potential energy surface of the neutral thymine–water complex by a molecular dynamics/quenching technique, were taken from a previous study of Hobza et al.<sup>23</sup> Structures were then reoptimized at MP2 level with the 6-31G\* basis set, and vibrational frequencies were computed at the same level to ensure the minimum character of the stationary points. Three transition-state (TS) structures connecting pairs of minima were optimized at the same level of theory. Intrinsic reaction path (IRC) calculations<sup>40</sup> were performed to compute a minimum energy path passing through the seven (four minima and three TS) stationary points.

Different levels of theory (in particular basis sets) were used to study VB and DB anions of the thymine–water complex. In both cases, the frozen core approximation was used for correlated calculations, and VEA, AEA, and VDE were obtained from the supermolecular approach using the following relationships

$$VEA = E_{(T-H_2O)}^{(T-H_2O)} - E_{(T-H_2O)^-}^{(T-H_2O)} \quad (1)$$

$$AEA = E_{(T-H_2O)}^{(T-H_2O)} - E_{(T-H_2O)^-}^{(T-H_2O)^-} \quad (2)$$

$$VDE = E_{(T-H_2O)^-}^{(T-H_2O)^-} - E_{(T-H_2O)}^{(T-H_2O)^-} \quad (3)$$

where the subscript indicates whether the energy has been computed for the neutral or anionic complex, and the superscript defines at what geometry the energy is evaluated. This also implies that the calculations of stationary points of the neutral complex were refined at the higher level of theory used for the anions, specified in the following subsections.

Resolution of the identity MP2 (RI-MP2) optimizations were carried out with the computer code Turbomole 4.7.<sup>41</sup> All of the remaining calculations were performed using Gaussian03.<sup>42</sup>

**2.1. Dipole-Bound Anions.** To describe dipole-bound electrons properly, standard basis sets (in our case 6-31+G\* and aug-cc-pVDZ<sup>43</sup>) have to be augmented with an additional set composed of very diffuse functions. The nonspherical character of the excess electron necessitates the inclusion of higher angular momentum functions. It has been shown previously<sup>44</sup> that the inclusion of S and P functions already accounts for more than 90% of the binding energy at the MP2 level of theory.

Therefore, only S and P additional diffuse sets were added. Within relatively broad margins, the exact position of the diffuse sets has little influence on the results.<sup>15,16,18,45</sup> Because the orbital occupied by a DB electron is centered outside the molecule toward the positive end of its dipole moment, it is common practice to place them there. In our calculations, the additional diffuse functions were placed on the atom closest to the positive end of the dipole moment of the neutral complex.

The additional S and P diffuse functions have exponents  $\alpha_i = \alpha_1 q^{i-1}$ ,  $i = 1 \dots n$ .<sup>45</sup> Three parameters have to be determined: the lowest exponent,  $\alpha_1$ , the progression parameter,  $q$ , and the length of the sequence (i.e., the number of additional S and P sets),  $n$ . To obtain these parameters, we followed the procedure developed by Gutowski et al.<sup>45</sup> The value of the highest exponent should be smaller than the exponent of the most diffuse function in the standard basis set by at least a factor of 2. In the present work, its value was obtained simply by halving the value of the smallest exponent appearing in the standard basis set.

The value of the progression parameter depends on the value of the dipole moment of the neutral molecule.<sup>45</sup> For molecules with dipole moments in the 3.0–4.5 D range,  $q$  adopts values between 3.0 and 5.0.<sup>11,45</sup> To increase the numerical stability and the efficiency of our calculations,<sup>18</sup> we utilized a value of  $q = 5.0$ . To determine the length of sequence  $n$ , SCF orbitals of the neutral complex were computed with the diffuse set present, and  $n$  was increased until the molecular orbital coefficients of the most diffuse sets were not dominant, that is, the extra diffuse basis set became saturated.<sup>45</sup>

Because electron correlation effects change the properties of DB anions significantly,<sup>8,11,45</sup> and because the computation of electronic affinities requires the use of size-extensive methods, geometry optimizations were performed at the MP2/aug-cc-pVDZX level (X indicates the additional diffuse basis set).

Assuming that the difference between CCSD(T) and MP2 energies exhibits only a small basis set dependency,<sup>46,47</sup> CCSD(T) energies can be approximated as

$$E_{\text{aug-cc-pVDZX}}^{\text{CCSD(T)}} = E_{\text{aug-cc-pVDZX}}^{\text{MP2}} + (E_{6-31+G^*X}^{\text{CCSD(T)}} - E_{6-31+G^*X}^{\text{MP2}}) \quad (4)$$

where  $E_{6-31+G^*X}^{\text{CCSD(T)}}$  and  $E_{6-31+G^*X}^{\text{MP2}}$  are computed at MP2/aug-cc-pVDZX geometries.

Because no substantial spin contamination was observed in any calculations of DB anions, unrestricted CCSD(T) and MP2 methods were used. To improve convergency, the HF/aug-cc-pVDZX orbitals of the neutral complex were used as a starting orbital guess.

Because of the negligible geometry difference between DB and neutral complexes, we assumed that zero point energy (ZPE) corrections are the same for DB and neutral complexes (as a check, we found that in the structure denoted below as D, ZPEs

of neutral and anionic thymine–water complexes differ by less than 2 meV).

**2.2. Valence-Bound Anions.** Because of the relatively high computational demands of MP2 calculations with the employed basis sets, the approximate resolution of the identity MP2 (RI-MP2) method<sup>48,49</sup> was used for geometry optimizations. In the RI-MP2 approximation, two-electron four-center integrals are replaced by linear combinations of two-electron three-center integrals, which are easier to compute, via the introduction of an auxiliary fitting basis set, and a lower number of integrals needs to be computed and stored.<sup>48–50</sup> This allows a speedup of RI-MP2 calculations compared with standard MP2 that depends on the details of the calculations but reaches 1 order of magnitude easily.<sup>48,50,51</sup> Regarding the accuracy, it has been shown on several systems that, with an accurate choice of the auxiliary fitting basis set, energies and structures computed with MP2 and RI-MP2 methods do not show significant differences.<sup>48,51,52</sup> In particular, interaction energies of selected H-bonded and stacked DNA base pairs, computed with MP2 and RI-MP2 methods, are almost identical,<sup>50</sup> and we showed in a previous contribution that the AEA of the VB thymine anion differs only marginally ( $\sim 1$  meV) when computed with MP2 and RI-MP2 methods.<sup>18</sup>

A procedure similar to that adopted in our previous study of isolated thymine<sup>18</sup> was applied to the geometry optimization of VB anions. Geometries of the neutral complex were used as starting structures and were first optimized at the RI-MP2/6-31G\* level. Subsequent optimizations were performed at the RI-MP2/aug-cc-pVTZ level. The preliminary optimizations with the 6-31G\* basis set converged to complexes characterized by a nonplanar ring, and the following optimizations at RI-MP2/aug-cc-pVTZ converged to the correct VB structures. In this way, we avoided artifacts of direct optimizations at the RI-MP2/aug-cc-pVTZ level, that tend to converge to higher energies, corresponding to hybrid dipole-bound–valence-bound structures.<sup>18</sup>

In the case of TS calculations, a proper choice of starting guess structures proved to be particularly important. Thymine atomic coordinates were taken from the RI-MP2/aug-cc-pVTZ optimized geometry of one of the two minima connected directly to the transition structure. The water molecule was initially placed in the same relative position to the thymine molecule as in the neutral TS structure (optimized at the same level of theory). Compatibly with minima calculations, final optimizations were performed at the RI-MP2/aug-cc-pVTZ level.

Complete basis set (CBS) MP2 energies were estimated using the extrapolation scheme developed by Helgaker et al.<sup>53,54</sup> utilizing Dunning's augmented correlation consistent basis sets of double- and triple- $\zeta$  quality:<sup>43</sup>

$$E_{\infty}^{\text{HF}} = E_{\text{aug-cc-pVDZ}}^{\text{HF}} + (E_{\text{aug-cc-pVTZ}}^{\text{HF}} - E_{\text{aug-cc-pVDZ}}^{\text{HF}})/0.760691 \quad (5)$$

$$E_{\infty}^{\text{MP2}} = E_{\text{aug-cc-pVDZ}}^{\text{MP2}} + (E_{\text{aug-cc-pVTZ}}^{\text{MP2}} - E_{\text{aug-cc-pVDZ}}^{\text{MP2}})/0.703704 \quad (6)$$

Because of the presence of a nonnegligible spin contamination ( $\langle \hat{S}^2 \rangle \approx 0.80$ ), single point energy calculations were performed for optimized structures with the spin-projected MP2 method (PMP2) with the aug-cc-pVDZ and aug-cc-pVTZ basis sets.<sup>18</sup> Because no substantial spin contamination was observed at the CCSD(T) level, unrestricted CCSD(T) was used in our calcula-



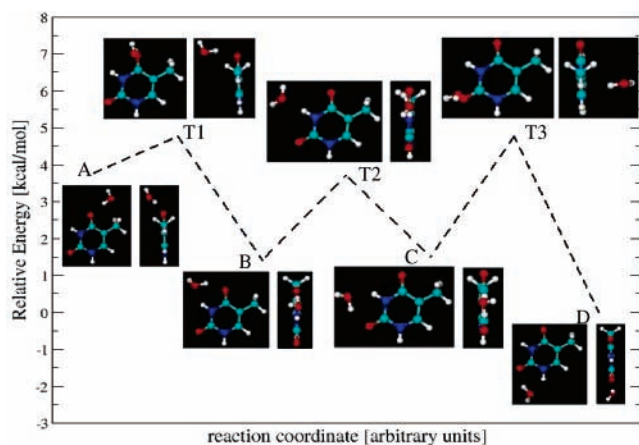


**Figure 2.** Relative energies and optimized geometries of stationary points of the neutral complex.

**TABLE 1: Relative Energies, Expressed in kcal/mol, of Neutral Complexes Computed at Different Levels of Theory**

complex	MP2			MP2+ $\Delta E_{CC}^a$		
	6-31G*	aug-cc-pVDZ	aug-cc-pVTZ	CBS	CBS	CBS+ZPE
A	6.13	4.19	4.30	4.36	4.24	3.77
B	1.57	1.65	1.57	1.53	1.53	1.40
C	1.98	1.86	1.84	1.84	1.69	1.50
D	0	0	0	0	0	0
T1	8.40	5.62	5.70	5.75	5.58	4.76
T2	5.58	4.52	4.68	4.76	4.67	3.70
T3	8.34	5.65	5.77	5.84	5.58	4.76

$$^a \Delta E_{CC} = E_{6-31+G^*}^{CCSD(T)} - E_{6-31+G^*}^{MP2}$$

tions. As explained above, CCSD(T) energies were extrapolated as follows:

$$E_{\infty}^{CCSD(T)} = E_{\infty}^{MP2} + (E_{6-31+G^*}^{CCSD(T)} - E_{6-31+G^*}^{MP2}) \quad (7)$$

Finally, because of the significant differences between neutral and VB optimized geometries, ZPE corrections, calculated at the RI-MP2/aug-cc-pVDZ level without the inclusion of any scaling factor, were added to computed energies. We notice at this point that, for both VB anions and neutral complexes, the ZPE values of the TS structures were computed without including the contribution of the single imaginary frequency.

### 3. Results and Discussion

**Neutral Complex.** Figure 2 shows the minima and transition-state structures for the neutral complex, optimized at the RI-MP2/aug-cc-pVTZ level. All structures are characterized by a planar thymine ring. In structures B–D, the water molecule interacts with thymine via  $O_w H_w \cdots O$  and  $NH \cdots O_w$  hydrogen bonds. The water hydrogen and oxygen atoms involved in the H bond are coplanar with the thymine molecule, whereas the second H atom is pointing out of the plane. Because of the presence of the methyl group, structure A is somewhat different because the water is positioned outside of the thymine plane, and one of the two H bonds is substituted by two weak  $CH \cdots O_w$  interactions.

Regarding transition-state geometries, it can be noticed that one hydrogen bond is always broken. In structures T1 and T3, the water molecule lies outside the thymine plane and is bound through a  $CO \cdots H_w$  H bond, whereas in structure T2 it is coplanar with the thymine and the H bond is  $NH \cdots O_w$ .

Table 1 shows energies of the stationary points relative to the lowest minimum at different levels of theory. As expected,

larger basis sets reduce the size of the energy barriers between adjacent minima. Moreover, smaller basis sets, like 6-31G\*, consistently overestimate the energy of complex A. This is due to the fact that the water molecule lies outside the thymine ring plane; therefore, higher angular momentum basis sets are required to describe the water–thymine interaction energy correctly.

A set of six IRC calculations, two for every TS structure, have been performed to ensure that minima and TS are connected by a single minimum energy path. Because of the high computational demand, calculations were performed at the MP2/6-31G\* level. Figure 3 shows the resulting path. The situation is, however, somewhat more complex than it may appear. Because of the high number of degrees of freedom of the system and symmetry properties, more isoenergetic isomers of the stationary points exist. For example, the IRC branch connecting structure T2 with minimum C converged to a different, isoenergetic structure than the branch connecting transition point, T3, with the same minimum, C (see Figure 4). The minimum energy path is therefore not unique because some bifurcations<sup>55</sup> are present.

**Valence-Bound Anion.** Figure 5 shows the geometries of the VB anion stationary points. As expected,<sup>18,37,38,56</sup> relaxation of the structure upon electron attachment leads to major structural changes. The thymine ring of the anion complex is puckered significantly, and, in minimum structures the weaker hydrogen bond between water and thymine is broken, leading to the creation of electron-deficient areas where the excess electron can attach.<sup>36</sup> The puckering of the ring implies less severe antibonding interactions, and, therefore, stabilization of the anion.<sup>38</sup> The H-bond pattern remains unchanged in structures T1 and T3, whereas in T2 the  $NH \cdots O_w$  bond is replaced by two  $CO \cdots H_w$  bonds. We notice that the water molecule, in structure T3, moves out of the thymine plane upon electron attachment.

The relative energies of the different structures are reported in Table 2. The energy barriers between structures A and B and C and D are lower than those in the neutral complex (less than 1 kcal/mol). The stability order of minimal structures is different than that for the neutral complex,<sup>37,38</sup> structure B now being the lowest in energy.

Table 3 reports the computed values of AEAs and VDEs of minimum structures. At the PMP2/aug-cc-pVDZ and PMP2/aug-cc-pVTZ levels, three and two complexes, respectively, still have negative adiabatic electron affinities. The addition of ZPE corrections, computed at the RI-MP2/aug-cc-pVDZ level, combined with the extrapolation to the complete basis set limit, results in positive AEAs for all of the structures. The inclusion of single-point CCSD(T) corrections computed with the 6-31+G\* basis set ( $\Delta E_{CCSD(T)} = E_{6-31+G^*}^{CCSD(T)} - E_{6-31+G^*}^{MP2}$ ) further increases these values by about 20 meV; the final values of AEAs range from 66 to 287 meV. VDEs follow a similar trend, and our best estimates range from 698 meV for the least stable structure to 977 meV for the most stable one.

Schiedt et al. obtained, via electron spectroscopy experiments, a value of 0.3 eV for AEA and 0.9 eV for VDE of the thymine–water complex.<sup>34</sup> Considering that the authors claim an accuracy around 0.1 eV, our results are in excellent agreement with the reported experimental values. In analogy to the uracil–water complex,<sup>37</sup> we suggest that the presence of several isomers may account for the broad shape of the peaks of the recorded spectra.

A second comparison can be done with the results of Ortiz et al.<sup>37</sup> and Gutowski et al.,<sup>38</sup> who performed ab initio calculations for several uracil–water minima. The similarity of the systems allows one to make a one to one correspondence

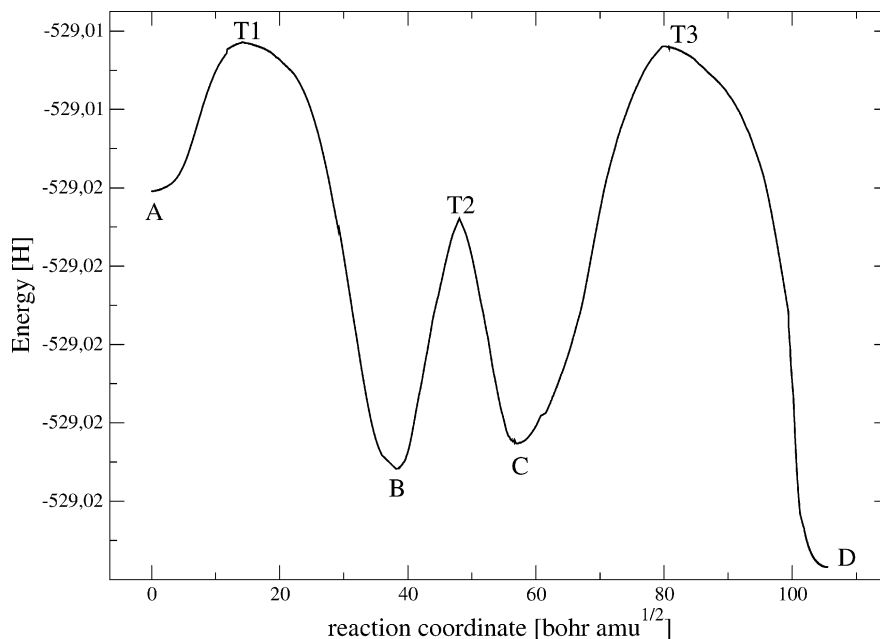


**Figure 3.** IRC path in the potential energy surface of the neutral system.

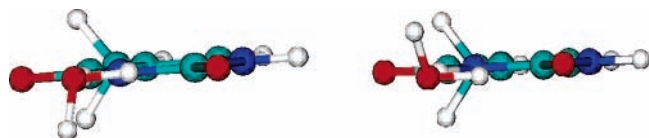


**Figure 4.** Geometries of the two isomers of structure C as obtained at the end of two different IRC branches.

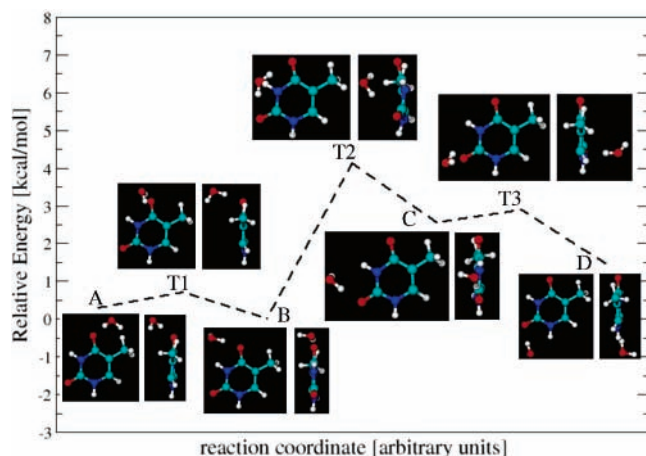


**Figure 5.** Relative energies and optimized geometries of stationary points of the valence-bound anion.

between the four minimum structures (see Table 3). The fact that both VDEs and AEAs are larger for the T–H<sub>2</sub>O complex in comparison to the results of U–H<sub>2</sub>O complex by Ortiz et al.<sup>37</sup> may appear contradictory because increasing the system size should result in lowering of the electronic affinities.<sup>57</sup> This is, however, explained easily by the fact that we used a higher level of theory in the present calculations. As a confirmation, the AEA of the less-stable (with respect to electron detachment) U–H<sub>2</sub>O structure (D) was recomputed at the same level as we employed for the T–H<sub>2</sub>O complex. Consequently, we obtained an AEA of 132 meV, which is appreciably higher than the –7 meV value reported in ref 37.

The electron binding energies obtained by Gutowski et al.<sup>38</sup> are considerably higher than our estimates, but the authors found that the level of theory used, B3LYP/6-31++G\*\*(5d), over-

**TABLE 2: Relative Energies, Expressed in kcal/mol, of Neutral Complexes, Valence-Bound and Dipole-Bound Anions<sup>a</sup>**

complex	neutral	VB anion	DB anion
	MP2/CBS+ $\Delta E_{cc}$ <sup>b</sup>	PMP2/CBS+ $\Delta E_{cc}$ <sup>b</sup>	MP2/aug-cc-pVDZX+ $\Delta E_{cc}$ <sup>c</sup>
A	4.24 (3.77)	0.45 (0.30)	2.91 <sup>d</sup> (2.44) <sup>d</sup>
B	1.53 (1.40)	0	0.58 (0.45)
C	1.69 (1.50)	2.78 (2.54)	0.57 (0.38)
D	0	1.49 (1.44)	0
T1	5.58 (4.76)	1.22 (0.69)	4.90 (4.08)
T2	4.67 (3.70)	4.34 (4.13)	4.52 (3.55)
T3	5.58 (4.76)	3.53 (2.88)	5.30 (4.48)

<sup>a</sup> Values in brackets are corrected for ZPE. <sup>b</sup>  $\Delta E_{cc} = E_{6-31+G^*}^{CCSD(T)} - E_{6-31+G^*}^{MP2}$ . <sup>c</sup>  $\Delta E_{cc} = E_{6-31+G^*X}^{CCSD(T)} - E_{6-31+G^*X}^{MP2}$ . <sup>d</sup> Calculated at A geometry.

**TABLE 3: Comparison of AEAs and VDEs of Valence-Bound Anions of T–H<sub>2</sub>O and U–H<sub>2</sub>O Systems<sup>a</sup>**

complex	T–H <sub>2</sub> O (PMP2/CBS+ $\Delta E_{cc}$ <sup>b</sup> )			U–H <sub>2</sub> O		
	AEA	AEA+ZPE	VDE	AEA+ZPE <sup>c</sup>	VDE <sup>c</sup>	VDE <sup>d</sup>
A	193	287	977	214	900	1188
B	95	198	871	117	830	1100
C	–16	94	759	32	720	1089
D	–44	66	698	–7	630	955

<sup>a</sup> Values are in MeV. VEAs are not given because an anion in the geometry of neutral is not bound. <sup>b</sup>  $\Delta E_{cc} = E_{6-31+G^*}^{CCSD(T)} - E_{6-31+G^*}^{MP2}$ . <sup>c</sup> Results are taken from ref 37 and were computed at the PMP2/6-311++G(2df,2p) level. <sup>d</sup> Results are taken from ref 38 and were computed at the B3LYP/6-31++G\*\*(5d) level.

estimates the VDE of bare uracil by about 200 meV, and a similar error may affect the uracil–water complex results as well.

Adamowicz et al. found a VB structure with the water molecule placed above the thymine ring which, however, has a large negative AEA (–250 meV at the MP2/aug-cc-pVDZ level),<sup>56</sup> and a structure with the excess electron positioned between uracil and water, which is very high in energy.<sup>39</sup>

Finally, Figure 6a shows the HOMO of one of the minimum VB structure (C). The electron is localized mainly on the thymine molecule, a fact that may account for the stabilization

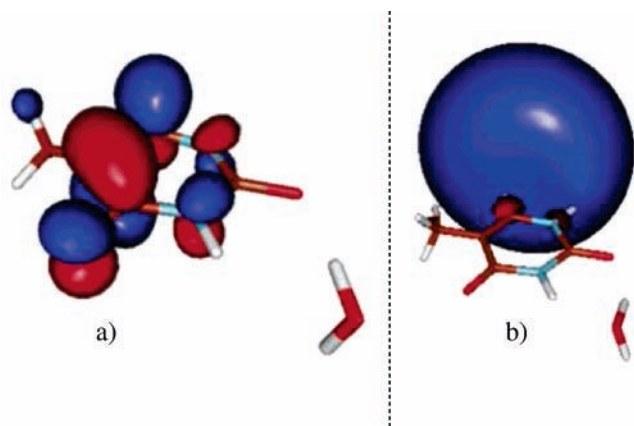


**Figure 6.** Highest occupied molecular orbital (HOMO) in valence-bound (a) and dipole-bound (b) thymine–water complex, structure C, obtained at the MP2/aug-cc-pVDZ level. The isocontour surface is drawn at a value of 0.04 for the VB and 0.008 for the DB anions.

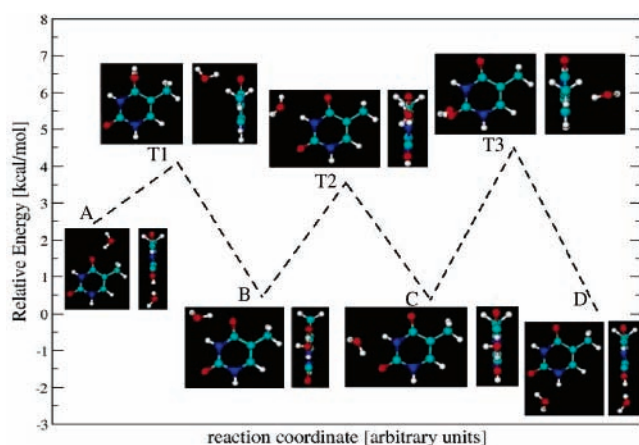


**Figure 7.** Relative energies and optimized geometries of stationary points of the dipole-bound anion.

**TABLE 4: Dipole Moments of Neutral Complexes Computed at the MP2/aug-cc-pVDZ Level**

complex	dipole moment (D)
A	4.01
B	4.78
C	5.34
D	3.44
T1	4.97
T2	2.49
T3	3.94

of VB anions compared with DB anions because of solvation by water. As suggested by Adamowicz et al.,<sup>56</sup> the interaction of the water molecule with the more localized, covalently attached electron is stronger than that in the case of the very diffuse DB electron (Figure 6b).

**Dipole-Bound Anion.** Figure 7 shows the optimized structures of the DB anion complex. Table 4 reports the values of the dipole moment for all neutral complexes, computed at the MP2/aug-cc-pVDZ level. Optimization at the MP2/aug-cc-pVDZX level led to geometries very close to those of the neutral complex. Consequently, isomerization energies (Table 2) are similar to those observed for the neutral molecule. In case of structure A, we did not find a DB anion with the water molecule positioned outside the thymine ring plane, as in the corresponding neutral complex. Energy minimization pushed the water back to the plane, and a DB anion structure (see Figure 8) was found. Subsequently, a planar neutral structure,  $\tilde{A}$ , was optimized, and resulted very close in energy (few meV) to structure A.

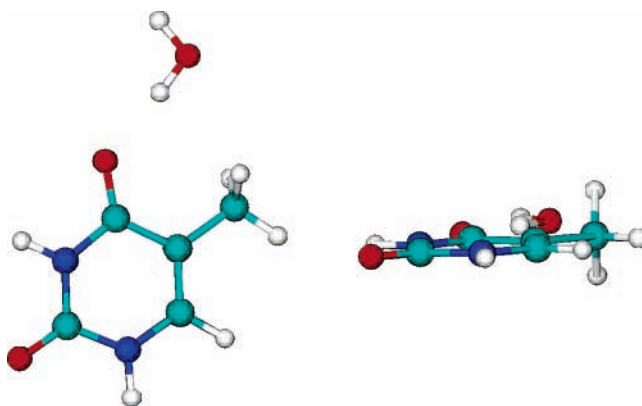


**Figure 8.** Geometry of the optimized dipole-bound anion structure  $\tilde{A}$ .

**TABLE 5: AEAs, VDEs, and VEAs of the Dipole-Bound Anion of T–H<sub>2</sub>O Complexes and AEA of the Dipole-Bound Anion of the U–H<sub>2</sub>O System<sup>a</sup>**

complex	T–H <sub>2</sub> O (MP2/aug-cc-pVDZX)+ $\Delta E_{CC}$ <sup>b</sup>			U–H <sub>2</sub> O
	AEA	VDE	VEA	AEA <sup>c</sup>
$\tilde{A}$	57	70	50	
B	50	60	41	36
C	58	69	48	44
D	8	10	8	6

<sup>a</sup> Values are in MeV. <sup>b</sup>  $\Delta E_{CC} = E_{6-31+G^*X}^{CCSD(T)} - E_{6-31+G^*X}^{MP2}$  <sup>c</sup> Results are taken from ref 35 and were computed at the MP2/6-31+G\***X**//SCF/6-31+G\***X** level.

The values of AEAs and VDEs (Table 5) are consistently lower than those of the corresponding VB complexes, a finding that is compatible with experiments on U–H<sub>2</sub>O<sup>13</sup> and T–H<sub>2</sub>O<sup>34</sup> complexes, in which only VB anions were observed.

Our results can be compared (see Table 5) to previous theoretical calculations of Adamowicz et al.<sup>35</sup> on the U–H<sub>2</sub>O complex. The authors located three minima at the MP2/6-31+G\***X**//HF/6-31+G\***X** level. Because of the higher level of theory used, our values of electron binding energies are slightly larger than those computed for the U–H<sub>2</sub>O complex. We obtained AEAs in the 8–57 meV range for the different structures. VDEs and VEAs are slightly (few meV) higher and lower, respectively, than the corresponding AEAs.

**Influence of Electron Attachment on the PES.** As explained in the introductory section, one of the goals of this study is to map the PES of both neutral and anionic thymine–water systems. In the neutral complex (Figure 2), energy barriers between the two adjacent minima that are lowest in energy are too high to allow for a significant thermal motion of the water molecule between the two structures at room temperature. Because of the negligible geometry relaxation upon electron attachment and weak electron binding, a similar shape of the PES is observed for DB anions (Figure 7). However, we notice that, because of the difference in AEA between structure C and D, these two minima are now separated by a energy barrier of only 0.38 kcal/mol.

In VB anions (Figure 5), the energy barriers between adjacent minima A–B and C–D are lower than in the neutral complex, and the energy barrier between the two lowest energy minima (A and B) is only 0.3 kcal/mol high. Therefore, in both VB and DB anions, at ambient conditions, a significant delocalization of the water molecule is expected, particularly in the region between the two low-lying structures (A and B for VB, and C and D for DB anions).



#### 4. Conclusions

In the present work we have studied the onset of solvation of thymine anions and the influence of water on the stability of DB and VB states. We have located four minima and three transition states on the thymine–water potential energy surface. We have considered the neutral complex and two different anionic forms, dipole- and valence-bound anions. Using high-level *ab initio* calculations, vertical and adiabatic electronic affinities have been computed for minimum structures.

The main results can be summarized as follows: (1) Extrapolation to the complete basis set limit and accounting for the ZPE is necessary in order to obtain positive values of AEAs for each of the considered VB anion geometries. The resulting numbers fall between 66 and 287 meV for AEAs, and 698–977 meV for VDEs. A good agreement is obtained, whenever available, with previous experimental and theoretical studies. Attachment of a VB electron to thymine leads to a significant geometry perturbation: the thymine ring is appreciably puckered, and the hydrogen bond structure is modified. The PES for the VB anion is different from the PES of the neutral complex because the stability order of the minima is modified. Moreover, the energy barriers between adjacent minima A–B and C–D are lowered. In particular, the two lowest energy minima, structures A and B, are now separated by a barrier only 0.3 kcal/mol high, so at ambient condition a considerable delocalization of the water molecule is expected between these two structures. (2) For DB anions, the optimized geometries are similar to those of the parent neutral complex. Consequently, AEAs, VDEs, and VEAs are very close to each other, and they are in the 8–70 meV range. The PES of the DB and neutral thymine are similar to each other, as, with the exception of structures B and C (that, however, differ only by a small fraction of kcal/mol in both anionic and neutral complexes), the stability order of the minima remain unchanged. In analogy with the VB anions, we observed that the energy barrier between the two lowest energy minima is lowered to 0.38 kcal/mol, so the same delocalization of the water molecule, noticed for VB anions, is expected.

An isolated thymine interacting with a single water molecule and an electron is an interesting system in its own right. However, it is of course far from the real situation in DNA; therefore, care should be taken when making generalized conclusions. In a nucleotide, the N1 position is blocked by the bond to the sugar. This bond is often excluded in calculations by adding a methyl group. We did not follow this approach because we wanted to compare our results with previous theoretical and experimental works that were done on non-methylated systems. Moreover, the O4 and N3–H positions are blocked by the hydrogen bonds to adenine, which excludes the presence of the water molecule in position B (see Figure 1).

Database studies of hydrated DNA X-ray structures show that pyrimidines usually have a single associated water molecule, which can form a hydrogen bond to another base, often via a second water molecule (water bridges).<sup>58,59</sup> Consistent with previous findings of Schneider et al.,<sup>60</sup> this water molecule can be found either in the major groove edge (structure A – O4 water), or in the minor groove edge (structures C and D – O2 water), where it takes part in the so-called spine of hydration.<sup>58</sup> Water molecules in the major groove were observed, because of their high mobility caused by the presence of large hydrophobic thymine methyl groups, only in high-resolution, low-temperature B-DNA structures, while the minor groove base hydration is much more localized.<sup>58,60</sup>

In B-DNA crystals, water molecules are also found in a position between structure D and the methyl group.<sup>60</sup> In this configuration, the water is weakly hydrogen bonded to the C–H of the methyl group and stabilized by the interaction with the phosphate group. Such a minimum energy structure was not found in our calculations. Moreover, hydration of DNA bases depends on the form of DNA, as was demonstrated clearly for guanine in Z-DNA and in B-DNA.<sup>61</sup> Generally, it is difficult in an X-ray crystallographic analysis to identify the H atoms, but recently neutron diffraction experiments succeeded in determining most hydrogen atomic positions in the hydrated decameric d(CCATTAATGG)<sub>2</sub> duplex.<sup>59</sup>

Finally, the negatively charged phosphate group in DNA is compensated by the presence of cations. This very likely leads to changes in the local electric field, which may consequently influence the position of the electron and its binding energy. The creation of valence-bound anions (dipole-bound anions of DNA bases are not relevant to a biological system<sup>62</sup>) is accompanied by significant ring puckering of the planar base. In addition to aromatic stabilization, the planarity of the neutral base ring is stabilized by the stacking and hydrogen-bonding interactions with neighboring bases, which would also affect the adiabatic electron affinity. Moreover, the character of an excess electron in DNA is still a matter of controversy;<sup>63</sup> it is not clear whether the surrounding polar medium leads to the delocalization of charge in DNA over adjacent base pairs<sup>64,65</sup> or not.<sup>66,67</sup> More research is certainly needed to establish the behavior of excess electrons in DNA. Studies of electron attachment to isolated and microhydrated DNA bases represent one of the possible first steps in this direction.

**Acknowledgment.** Support from the Granting Agency of the Academy of Sciences of the Czech Republic (Grant no. IAA400400503) is gratefully acknowledged. We are grateful to Martin Kabelac for providing the structures resulting from MD/quenching optimization.

#### References and Notes

- (1) Simons, J.; Jordan, K. D. *Chem. Rev.* **1987**, *87*, 535.
- (2) Fermi, E.; Teller, E. *Phys. Rev.* **1947**, *72*, 399.
- (3) Garrett W. R. *Phys. Rev. A* **1971**, *3*, 961.
- (4) Crawford, H. O.; Dalgarno, A. *Chem. Phys. Lett.* **1967**, *91*, 279.
- (5) Desfrancois, C.; AbdoulCarime, H.; Schermann, J. P. *Int. J. Mod. Phys. B* **1996**, *10*, 1339.
- (6) Gutowski, M.; Skurski, P. *Recent Res. Dev. Phys. Chem.* **1999**, *3*, 245.
- (7) Jordan, K.; Wang, F. *Annu. Rev. Phys. Chem.* **2003**, *54*, 367.
- (8) Gutowski, M.; Skurski, P.; Boldyrev, A. I.; Simons, J.; Jordan, K. D. *Phys. Rev. A* **1996**, *54*, 1906.
- (9) Gutowski, M.; Skurski, P. *J. Phys. Chem. B* **1997**, *101*, 9143.
- (10) Gutowski, M.; Skurski, P.; Jordan, K.; Simons, J. *Int. J. Quantum Chem.* **1997**, *64*, 183.
- (11) Gutowski, M.; Jordan, K. D.; Skurski, P. *J. Phys. Chem. A* **1998**, *102*, 2624.
- (12) Svozil, D.; Jungwirth, P.; Havlas, Z. *Collect. Czech. Chem. Commun.* **2004**, *69*, 1395.
- (13) Hendricks, J. H.; Lyapustina, S. A.; deClercq, H. L.; Snodgrass, J. T.; Bowen, K. H. *J. Chem. Phys.* **1996**, *104*, 7788.
- (14) Desfrancois, C.; Periquet, V.; Bouteiller, Y.; Schermann, J. P. *J. Phys. Chem. A* **1998**, *102*, 1274.
- (15) Oyler, N. A.; Adamowicz, L. *J. Phys. Chem.* **1993**, *97*, 11122.
- (16) Oyler, N. A.; Adamowicz, L. *Chem. Phys. Lett.* **1994**, *219*, 223.
- (17) Sevilla, M. D.; Besler, B.; Colson, A. O. *J. Phys. Chem.* **1995**, *99*, 1060.
- (18) Svozil, D.; Frigato, T.; Havlas, Z.; Jungwirth, P. *Phys. Chem. Chem. Phys.* **2005**, *7*, 840.
- (19) Sommerfeld, T. *J. Phys. Chem. A* **2004**, *108*, 9150.
- (20) van Mourik, T.; Price, S. L.; Clary, D. C. *J. Phys. Chem. A* **1999**, *103*, 1611.
- (21) van Mourik, T.; Benoit, D. M.; Price, S. L.; Clary, D. C. *Phys. Chem. Chem. Phys.* **2000**, *2*, 1281.
- (22) van Mourik, T. *Phys. Chem. Chem. Phys.* **2001**, *3*, 2886.

- (23) Rejnek J.; Hanus, M.; Kabelac, M.; Ryjacek, F.; Hobza, P. *Phys. Chem. Chem. Phys.* **2005**, *7*, 2006.
- (24) Nguyen, M. T.; Chandra, A. K.; Zeegers-Huyskens, T. *Faraday Trans.* **1998**, *94*, 1277.
- (25) Chandra, A. K.; Nguyen, M. T.; Zeegers-Huyskens, T. *J. Phys. Chem. A* **1998**, *102*, 6010.
- (26) Gadre, S. R.; Babu, K.; Rendell, A. P. *J. Phys. Chem. A* **2000**, *104*, 8976.
- (27) Gaigeot, M. P.; Ghomi, M. *J. Phys. Chem. B* **2001**, *105*, 5007.
- (28) Kryachko, E. S.; Nguyen, M. T.; Zeegers-Huyskens, T. *J. Phys. Chem. A* **2001**, *105*, 1934.
- (29) Di Laudo, M. Whittleton, S. R.; Wetmore, S. D. *J. Phys. Chem. A* **2003**, *107*, 10406.
- (30) Hu, X.; Li, H.; Liang, W.; Han, S. J. *J. Phys. Chem. B* **2004**, *108*, 12999.
- (31) Hu, X.; Li, H.; Liang, W.; Han, S. J. *J. Phys. Chem. B* **2005**, *109*, 5935.
- (32) Gaigeot, M. P.; Sprik, M. *J. Phys. Chem. B* **2004**, *108*, 7458.
- (33) Hendricks, J. H.; Lyapustina, S. A.; de Clercq, H. L.; Bowen, K. H. *J. Chem. Phys.* **1998**, *108*, 8.
- (34) Schiedt, J.; Weinkauff, R.; Neumark, D. M.; Schlag, E. W. *Chem. Phys.* **1998**, *239*, 511.
- (35) Smets, J.; McCarthy, W. J.; Adamowicz, L. *J. Phys. Chem.* **1996**, *100*, 14655.
- (36) Smets, J.; Smith, D. M. A.; Elkadi, Y.; Adamowicz, L. *J. Phys. Chem. A* **1997**, *101*, 9152.
- (37) Dolgounitcheva, O.; Zakrzewski, V. G.; Ortiz, J. V. *J. Phys. Chem. A* **1999**, *103*, 7912.
- (38) Haranczyk, M.; Bachorz, R.; Rak, J.; Gutowski, M.; Radisic, D.; Stokes, S. T.; Nilles, J. M.; Bowen, K. T. *J. Phys. Chem. B* **2003**, *107*, 7889.
- (39) Jalbout, A. F.; Hall-Black, C. S.; Adamowicz, L. *Chem. Phys. Lett.* **2002**, *354*, 128.
- (40) Fukui, K. *Acc. Chem. Res.* **1981**, *14*, 363.
- (41) Ahlrichs, R.; Bar, M.; Haser, M.; Horn, H.; Kolmel, C. *Chem. Phys. Lett.* **1989**, *162*, 165.
- (42) Frisch, M. J.; Trucks, G. W.; Schlegel, H. B.; Scuseria, G. E.; Robb, M. A.; Cheeseman, J. R.; Montgomery, J. A., Jr.; Vreven, T.; Kudin, K. N.; Burant, J. C.; Millam, J. M.; Iyengar, S. S.; Tomasi, J.; Barone, V.; Mennucci, B.; Cossi, M.; Scalmani, G.; Rega, N.; Petersson, G. A.; Nakatsuji, H.; Hada, M.; Ehara, M.; Toyota, K.; Fukuda, R.; Hasegawa, J.; Ishida, M.; Nakajima, T.; Honda, Y.; Kitao, O.; Nakai, H.; Klene, M.; Li, X.; Knox, J. E.; Hratchian, H. P.; Cross, J. B.; Bakken, V.; Adamo, C.; Jaramillo, J.; Gomperts, R.; Stratmann, R. E.; Yazyev, O.; Austin, A. J.; Cammi, R.; Pomelli, C.; Ochterski, J. W.; Ayala, P. Y.; Morokuma, K.; Voth, G. A.; Salvador, P.; Dannenberg, J. J.; Zakrzewski, V. G.; Dapprich, S.; Daniels, A. D.; Strain, M. C.; Farkas, O.; Malick, D. K.; Rabuck, A. D.; Raghavachari, K.; Foresman, J. B.; Ortiz, J. V.; Cui, Q.; Baboul, A. G.; Clifford, S.; Cioslowski, J.; Stefanov, B. B.; Liu, G.; Liashenko, A.; Piskorz, P.; Komaromi, I.; Martin, R. L.; Fox, D. J.; Keith, T.; Al-Laham, M. A.; Peng, C. Y.; Nanayakkara, A.; Challacombe, M.; Gill, P. M. W.; Johnson, B.; Chen, W.; Wong, M. W.; Gonzalez, C.; Pople, J. A. *Gaussian 03*, revision C.02; Gaussian, Inc.: Wallingford, CT, 2004.
- (43) Kendall, R.; Dunning, T.; Harrison, R. *J. Chem. Phys.* **1992**, *96*, 6796.
- (44) Skurski, P.; Gutowski, M. *J. Chem. Phys.* **1998**, *108*, 6303.
- (45) Skurski, P.; Gutowski, M.; Simons, J. *Int. J. Quantum Chem.* **2000**, *80*, 1024.
- (46) Koch, H.; Fernandez, B.; Christiansen, O. *J. Chem. Phys.* **1998**, *108*, 2784.
- (47) Jurecka, P.; Hobza, P. *Chem. Phys. Lett.* **2002**, *365*, 89.
- (48) Feyereisen, M.; Fitzgerald, G.; Komornicki, A. *Chem. Phys. Lett.* **1993**, *208*, 359.
- (49) Vahtras, O.; Almlöf, J.; Feyereisen, M. W. *Chem. Phys. Lett.* **1993**, *213*, 514.
- (50) Jurecka, P.; Nachtigall, P.; Hobza, P. *Phys. Chem. Chem. Phys.* **2001**, *3*, 4578.
- (51) Bernholdt, D.; Harrison, R. *Chem. Phys. Lett.* **1996**, *250*, 477.
- (52) Feller, D.; Apra, E.; Nichols, J.; Bernholdt, D. *J. Chem. Phys.* **1996**, *105*, 1940.
- (53) Halkier, A.; Helgaker, T.; Jorgensen, P.; Klopper, W.; Olsen, J. *Chem. Phys. Lett.* **1999**, *302*, 437.
- (54) Helgaker, T.; Klopper, W.; Koch, H.; Noga, J. *J. Chem. Phys.* **1997**, *106*, 9639.
- (55) Quapp, W. *J. Mol. Struct.* **2004**, *695*, 95.
- (56) Morgado, C. A.; Pichugin, K. Y.; Adamowicz, L. *Phys. Chem. Chem. Phys.* **2004**, *6*, 2758.
- (57) Desfrancois, C.; Abdoul-Carime, H.; Carles, S.; Periquet, V.; Scherman, J. P.; Smith, D. A. M.; Adamowicz, L. *J. Chem. Phys.* **1999**, *110*, 11876.
- (58) Neidle, S. *Nucleic Acid Structure and Recognition*; Oxford University Press: Oxford, U.K., 2002.
- (59) Arai, S.; Chatake, T.; Ohhara, T.; Kurihara, K.; Tanaka, I.; Suzuki, N.; Fujimoto, Z.; Mizuno, H.; Niimura, N. *Nucl. Acids Res.* **2005**, *33*, 3017.
- (60) Schneider, B.; Berman, H. M. *Biophys. J.* **1995**, *69*, 2661.
- (61) Schneider, B.; Cohen, D. M.; Schleifer, L.; Srinivisan, A. R.; Olson, W. K.; Berman, H. M. *Biophys. J.* **1993**, *65*, 2291.
- (62) Sevilla, M. D.; Besler, B.; Colson, A. O. *J. Phys. Chem.* **1994**, *98*, 2215.
- (63) Kurnikov, I. V.; Tong, G. S. M.; Madrid, M.; Beratan, D. N. *J. Phys. Chem. B* **2002**, *106*, 7.
- (64) Conwell, E. M.; Basko, D. M. *J. Am. Chem. Soc.* **2001**, *123*, 11441.
- (65) Basko, D. M.; Conwell, E. M. *Phys. Rev. Lett.* **2002**, *88*, 098102.
- (66) Voityuk, A. A. *J. Chem. Phys.* **2005**, *122*, 204904.
- (67) Voityuk, A. A. *J. Phys. Chem. B* **2005**, *109*, 10793.